

# Absence of the P2X<sub>7</sub> Receptor Alters Leukocyte Function and Attenuates an Inflammatory Response

Jeffrey M. Labasi,\* Nina Petrushova,\* Carol Donovan,\* Sandra McCurdy,\* Paul Lira,\* Mary M. Payette,<sup>†</sup> William Brissette,\* Joan R. Wicks,<sup>†</sup> Laurent Audoly,\* and Christopher A. Gabel<sup>1\*</sup>

When challenged with extracellular ATP, leukocytes respond and activate processes attributed to the P2X<sub>7</sub> receptor (P2X<sub>7</sub>R), an unusual ligand-gated ion channel. To prove P2X<sub>7</sub>R involvement, blood samples from P2X<sub>7</sub>R-deficient mice were characterized. Monocytes and lymphocytes associated with wild-type blood responded to ATP and underwent volume/shape changes and shed L-selectin. In contrast, leukocytes from P2X<sub>7</sub>R-deficient animals demonstrated no change in physical properties or L-selectin expression following ATP challenge. Blood stimulated with LPS or ATP individually generated minimal quantities of the leaderless polypeptide IL-1 $\beta$ , but sequential treatment of wild-type, but not P2X<sub>7</sub>R-deficient, blood with LPS and ATP yielded large amounts of cell-free cytokine. Based on these differences, wild-type and P2X<sub>7</sub>R-deficient animals were compared following induction of monoclonal anti-collagen-induced arthritis. Ab-treated wild-type animals subsequently challenged with LPS developed inflamed, swollen paws; their joint cartilage demonstrated lesions, loss of proteoglycan content, and the presence of collagen degradation products. P2X<sub>7</sub>R-deficient animals subjected to the same challenge were markedly less affected; both the incidence and severity of disease were reduced. These data indicate that ATP does act via the P2X<sub>7</sub>R to affect leukocyte function and that the P2X<sub>7</sub>R can serve as an important component of an in vivo inflammatory response. *The Journal of Immunology*, 2002, 168: 6436–6445.

The P2X<sub>7</sub> receptor (P2X<sub>7</sub>R)<sup>2</sup> is a ligand-gated ion channel that, like other members of the P2X family, mediates a nonselective cation conductance when stimulated with an appropriate ligand (1–4). However, prolonged ligation of the P2X<sub>7</sub>R leads to an unusual channel conductance state characterized by formation of pore-like structures permeable to large organic molecules such as ethidium bromide and YoPro Yellow (5–7). Opening of this pore in murine macrophages leads to complete depolarization of the membrane potential and, ultimately, cell death (8, 9). Recent investigations of the channel properties of other members of the P2X family have provided evidence that this type of pore-like activity may not be unique to the P2X<sub>7</sub>R (10, 11). Structure-function studies suggest that the extreme carboxyl-terminal domain of the P2X<sub>7</sub>R is necessary for pore formation, and this region of the polypeptide is absent in other P2X family members (1, 12). However, to date it remains unresolved as to whether the pore-like activity is an integral component of the P2X<sub>7</sub>R itself or is dependent on the association of this receptor with other cellular polypeptides (13, 14).

P2X<sub>7</sub>R activity is reported to exist in a limited number of cell types but is readily detectable in cells of hemopoietic lineage including monocytes, macrophages, and lymphocytes (15, 16). The physiological function of this receptor remains a subject of inves-

tigation, and a number of diverse activities have been proposed, including activation and maturation of T cells (17, 18), formation of giant cells (19, 20), killing of invading microorganisms in macrophages (21, 22), and activation of various signaling cascades (23–25). The receptor also has been proposed to serve as a regulator of inflammation, based on its ability to initiate posttranslational processing of leaderless cytokines such as IL-1 $\beta$  (26–28). When stimulated by an inflammatory insult such as LPS, monocytes, macrophages, and microglial cells generate large quantities of proIL-1 $\beta$  but release very little of the mature biologically active cytokine to the extracellular environment. However, efficient posttranslational processing of the procytokine molecules is rapidly engaged by treating the LPS-activated cells with ATP (26–29). Nucleoside triphosphate-induced cytokine processing is accompanied by a necessary K<sup>+</sup> efflux, activation of caspase-1 (the protease responsible for cleavage of proIL-1 $\beta$  to its mature form), and cell death (27–28, 30). LPS-activated peritoneal macrophages isolated from mice engineered to lack the P2X<sub>7</sub>R fail to generate mature IL-1 $\beta$  in response to ATP, confirming the role of P2X<sub>7</sub>R in this unusual biologic response (31).

ATP is considered to be a physiological ligand of the P2X<sub>7</sub>R (4, 16), but concentration requirements for this nucleoside triphosphate in normal tissue culture media can exceed millimolar values (1, 5). These high concentrations are reduced by removal of divalent cations from the medium, suggesting that the relevant ligand is ATP<sup>4-</sup> (5). Although the source of the ATP that engages the P2X<sub>7</sub>R in vivo remains to be established, in vitro studies have demonstrated that ATP can be released to the medium from degranulating platelets, dying cells, or viable cells via various transport processes (32–34). Nonetheless, the high ATP concentration requirements of the P2X<sub>7</sub>R remain problematic, and it is difficult to envision how millimolar levels of extracellular nucleotide triphosphate are achieved by any of the known ATP export mechanisms. A recent study using cocultures of astrocytes and microglia suggested that astrocytes released ATP in response to mechanical or

Departments of \*Antibacterials, Immunology, and Inflammation and <sup>†</sup>Drug Safety Evaluation, Pfizer Global Research and Development, Pfizer Inc., Groton, CT 06340  
Received for publication February 5, 2002. Accepted for publication April 10, 2002.

The costs of publication of this article were defrayed in part by the payment of page charges. This article must therefore be hereby marked *advertisement* in accordance with 18 U.S.C. Section 1734 solely to indicate this fact.

<sup>1</sup> Address correspondence and reprint requests to Dr. Christopher A. Gabel, Department of Antibacterials, Immunology, and Inflammation, Pfizer Global Research and Development, Pfizer, Inc., Groton, CT 06340. E-mail address: christopher\_a\_gabel@groton.pfizer.com

<sup>2</sup> Abbreviations used in this paper: P2X<sub>7</sub>R, P2X<sub>7</sub> receptor; KO, knockout; HiFAZ, heat-inactivated fetal serum with azide.

bradykinin activation in quantities sufficient to activate P2X<sub>7</sub>Rs on neighboring microglial cells (35). Thus, the context in which cells are exposed to ATP may influence ligand concentration requirements. In the present study we compare the ATP responsiveness of blood-derived leukocytes from wild-type and P2X<sub>7</sub>R-deficient mice, and demonstrate that absence of the receptor leads to loss of ATP-dependent leukocyte functions, including IL-1 $\beta$  production and L-selectin shedding. Moreover, wild-type and P2X<sub>7</sub>R-deficient mice are compared with respect to their susceptibility to monoclonal anti-collagen-induced arthritis, a model of inflammatory joint disease. Absence of the P2X<sub>7</sub>R is associated with less severe disease outcomes, indicating that the P2X<sub>7</sub>R can function as an integral component of an *in vivo* proinflammatory mechanism.

## Materials and Methods

### Mice

Generation of the P2X<sub>7</sub>R mice was described previously (31). These animals were maintained on a mixed genetic background (129/Ola  $\times$  C57BL/6  $\times$  DBA/2). Breeding P2X<sub>7</sub>R<sup>-/-</sup> males with P2X<sub>7</sub>R<sup>-/-</sup> females was used to maintain the colony of receptor-deficient animals. Likewise, genetically comparable wild-type animals were maintained by crossing homozygous animals. Mice used in the current studies generally were 12 wk of age.

### Cell Dyne assay

Wild-type and P2X<sub>7</sub>R-deficient mice were euthanized by CO<sub>2</sub> fixation and blood was collected into 1-ml syringes (containing 10 U/ml heparin) by cardiac puncture. Blood from individual animals was diluted 1/1 with RPMI 1640 medium containing 20 mM HEPES (pH 7.5), 100 U/ml penicillin, and 100  $\mu$ g/ml streptomycin. A total of 0.28 ml of each diluted blood sample was placed into a 1.5-ml capped tube and LPS (*Escherichia coli* serotype 055:B5; Sigma-Aldrich, St. Louis, MO) was added to some tubes to achieve a final concentration of 1  $\mu$ g/ml. These blood samples were incubated for 3 h at 37°C in a 5% CO<sub>2</sub> environment after which 5 mM effector (ATP, ADP, or UTP) was introduced to some tubes, and the incubation continued for an additional 2 h. At this point, samples were analyzed for leukocyte content by laser flow analysis using a Cell Dyne 3700 instrument (Abbott Laboratories, Abbott Park, IL) (36).

### FACS analysis for leukocyte L-selectin expression

Heparinized blood was isolated from wild-type and P2X<sub>7</sub>R-deficient animals as described above, samples from several individual animals of each genotype were combined, and 0.5 ml of the resulting pools was placed in 1.5-ml capped tubes. ATP was added to achieve a final concentration of 5 mM, and the samples were incubated at 37°C in a 5% CO<sub>2</sub> environment for 15 min. The nucleoside triphosphate (disodium salt from Sigma-Aldrich) was added from a 100 mM concentrate preneutralized to pH 7 by NaOH addition. MgCl<sub>2</sub> subsequently was added (final concentration of 20 mM) to quench the ATP-dependent response. At this point, the blood samples were split into two 0.2-ml aliquots and each was diluted with 1 ml of heat-inactivated fetal serum with azide (HiFAZ) reagent (PBS containing 0.02% sodium azide, 2% heat-inactivated FBS). These samples were subjected to centrifugation, and the resulting cell pellets were resuspended in 0.1 ml of HiFAZ reagent. Each of the duplicate samples received 5  $\mu$ l of allophycocyanin-labeled anti-CD62, after which one received 5  $\mu$ l of FITC-labeled anti-CD3 and the other received 5  $\mu$ l of PE-labeled anti-CD45; all Abs were obtained from BD PharMingen (San Diego, CA). Ab complexes were allowed to form at room temperature for 30 min, then the samples were diluted with 1 ml of HiFAZ reagent and cells was collected by centrifugation. Cell pellets were suspended in 2 ml of FACS lysing solution (BD Biosciences, San Jose, CA) and incubated for 10 min at room temperature to lyse RBCs. Leukocytes were recovered by centrifugation and washed once with 1 ml of HiFAZ reagent and suspended in 0.5 ml of this buffer. Samples were analyzed on a FACSCalibur instrument (BD Biosciences).

### Blood-based IL-1 assay

Heparinized blood (pooled samples from multiple animals of the same genotype) was dispensed into 96-well plates (0.12 ml/well) and diluted with an equal volume of RPMI 1640 medium containing 25 mM HEPES (pH 7.5), 1% FBS, 100 U/ml penicillin, and 100  $\mu$ g/ml streptomycin. LPS was introduced to some wells (final concentration of 1  $\mu$ g/ml), and the plates were incubated for 3 h at 37°C in a 5% CO<sub>2</sub> environment to promote proIL-1 $\beta$  synthesis. ATP subsequently was introduced to some wells to

achieve a final concentration of 5 mM, and the plates were incubated for an additional 2 h at 37°C. The plates then were subjected to centrifugation (700  $\times$  *g* for 10 min), the resulting plasma supernatants were harvested, and their content of murine IL-1 $\beta$  subsequently was determined by ELISA (Amersham Pharmacia Biotech, Piscataway, NJ).

### Peritoneal macrophage ATP response

Murine peritoneal macrophages were recovered as described previously (30). Isolated cells were washed with RPMI 1640 medium containing 5% heat-inactivated FBS, 100 U/ml penicillin, and 100  $\mu$ g/ml streptomycin, and then seeded into Natrix-coated six-well plates (BD Biosciences) at a density of 2  $\times$  10<sup>6</sup> cells/well. After an overnight incubation, media were removed, 1 ml of fresh RPMI 1640 medium containing 5% heat-inactivated FBS, 100 U/ml penicillin, 100  $\mu$ g/ml streptomycin, and 1  $\mu$ g/ml LPS was added to each well, and the cultures were incubated for 2 h at 37°C. ATP (5 mM) then was introduced, after which individual cultures were incubated for different periods of time before being photographed ( $\times$ 40 objective) by light microscopy or harvested for analysis of the distribution of  $\beta$ -hexosaminidase between the cell-associated and media fractions (27).

### mAb-induced arthritis

Arthritis was induced in mice using mAbs directed against type II collagen (37, 38). All procedures involving animals were approved by the Institutional Animal Care and Use Committee. The treatment consisted of i.p. injection (400  $\mu$ l) of a 10 mg/ml mAb mixture (Chemicon International, Temecula, CA) on day 0. Twenty-four hours later the mice were injected i.p. with LPS (100  $\mu$ l of a 0.25 mg/ml solution). During the subsequent 15 days, arthritis was assessed by the degree of swelling, redness, and ankylosis of the joints. All visual scores were combined into a score of 0–3 per paw and summed for a total score of 0–12 per animal. On day 15, hind paws were removed in some experiments for histological processing.

Both hind limbs (distal to the mid-femur) were collected and placed in 10% neutral buffered formalin for 24–48 h. The specimens were then decalcified in Immunocal (Decal Chemical, Congers, NY) for 48 h. The femorotibial (knee) and tibiotarsal (ankle) joints were cut in frontal and sagittal planes, respectively, dehydrated through graded alcohols, embedded in paraffin wax, and sectioned at 5  $\mu$ m. Sections were stained with safranin-O for acid mucopolysaccharides. For 9A4 immunohistochemistry (39), sections from the stifle joint were stained using DAKO ARK kit (DAKO, Carpinteria, CA) according to the manufacturer's directions. Ag retrieval was performed with Decal Solution (Biogenex, San Ramon, CA) at room temperature for 30 min. Endogenous peroxidase was blocked with 3% hydrogen peroxide followed by rinsing with distilled water. Ab 9A4 (2.3  $\mu$ g/ml) or a mouse isotype control IgG1 were biotinylated (DAKO biotinylation reagent) and incubated with tissue samples at room temperature for 45 min. Slides subsequently were washed and then incubated with streptavidin-HRP (DAKO) for 30 min. Binding of the primary Ab was detected by incubating the slides for 5 min in chromagen DAB<sup>+</sup> substrate-chromagen (DAKO), followed by counterstaining with hematoxylin.

Histologic evaluation on safranin-O sections was performed by a single blinded observer using a modified Mankin scale (40) as described below. This scale was developed to quantify changes in articular cartilage in humans with osteoarthritis, and was modified to reflect rodent size and to include synovial inflammation. This scale grades on a total composite scale of 0–17 and evaluates the severity of arthritis lesions based upon the following criteria: cartilage structural changes (0–6), cartilage cellularity changes (0–3), loss of safranin-O staining within the articular cartilage (0–4), and synovial inflammation and hyperplasia (0–4). 9A4 immunohistochemical staining was graded in reverse of the scale used for safranin-O (on a scale of 0–4); immunostaining was not included in the modified Mankin score but paralleled the loss of staining observed for glycosaminoglycans.

### Tetanus toxin challenge

Ten wild-type and 10 P2X<sub>7</sub> knockout (KO) mice were immunized with tetanus toxoid (NDC 49281-800-83; Aventis Pasteur, Swiftwater, PA); 0.1 ml was injected i.m. per mouse. On day 14, serum samples were collected by cardiac puncture and the mice were euthanized. These serum samples were tested for the presence of tetanus toxoid-specific IgG by ELISA as follows. Tetanus toxoid (10  $\mu$ l) was added to each well of 96-well Maxi-sorp plates (Nalge Nunc International, Naperville, IL) and incubated overnight in Dulbecco's PBS (D-PBS). The wells subsequently were washed three times with D-PBS containing 0.05% Tween 20. A solution of 5% BSA in D-PBS then was introduced to block remaining reactive sites, the plates were incubated for 2 h, and the wells again were washed three times. The collected serum samples were diluted in D-PBS, and 100- $\mu$ l aliquots were added to individual wells in triplicate of the tetanus toxin-coated

plates. Following a 2-h incubation, the serum-containing samples were removed, the wells were washed, and a solution of peroxidase-conjugated goat anti-mouse IgG (Jackson ImmunoResearch Laboratories, West Grove, PA) was added; the plates again were incubated for 2 h and then washed. Turbo TMB (Pierce, Rockford, IL) was added and the reaction was allowed to proceed for 20 min, after which sulfuric acid was added as a stop reagent. Reaction product was assessed with a ThermoMax plate reader (450 nm; Molecular Devices, Sunnyvale, CA).

## Results

### General characteristics of blood-borne leukocytes

Leukocyte populations reported to express the P2X<sub>7</sub>R include monocytes, T cells, and B cells (41–43), and ATP addition to human blood is known to promote physical alterations in specific leukocyte populations, possibly as a result of a P2X<sub>7</sub>R-mediated response (44). To determine whether murine blood leukocytes respond to extracellular ATP, a laser flow assay was formatted to allow simultaneous assessment of multiple cell types. When wild-type blood samples were treated with ATP, a decrease in the total number of leukocytes was observed (Fig. 1A). Treatment with LPS alone did not alter leukocyte numbers, nor did it augment the ATP-dependent response (Fig. 1A). Blood samples from P2X<sub>7</sub>R-deficient animals, in contrast, showed no decline in leukocyte numbers following ATP treatment (Fig. 1B); pretreatment with LPS did not uncover an ATP response. To identify cell types that responded to ATP, individual leukocyte populations were analyzed based on

their gating properties. Approximately 3.5% of total leukocytes associated with blood samples from wild-type animals displayed gating properties expected of monocytes. When treated with ATP (with or without prior LPS treatment), a near complete loss of monocytes was observed in wild-type blood samples (Fig. 1B). In this type of analysis a decline within a given population may result from an actual reduction in cell number (i.e., cell death) or from a change in cell morphology resulting in the affected cell demonstrating altered gating properties; in either case, a reduction in the number of cells gating as monocytes indicates that this population was affected by the extracellular stimulus. Loss of wild-type monocytes was not observed when ADP or UTP were substituted for ATP (Fig. 1E). Monocytes associated with blood samples derived from P2X<sub>7</sub>R-deficient animals comprised a similar overall percentage of the leukocyte population (3.5%) as found in wild-type blood samples. However, following treatment with ATP, monocyte numbers within the P2X<sub>7</sub>R-deficient samples remained constant (Fig. 1B).

Differences in lymphocyte (sum of both B and T) responsiveness also were observed between blood samples derived from wild-type and KO animals. Lymphocyte numbers declined >3-fold following treatment of wild-type blood samples with ATP, with or without prior LPS activation (Fig. 1C). In contrast, lymphocytes within blood samples derived from P2X<sub>7</sub>R KO animals were not affected by the ATP stimulus (Fig. 1C). Thus, like monocytes,

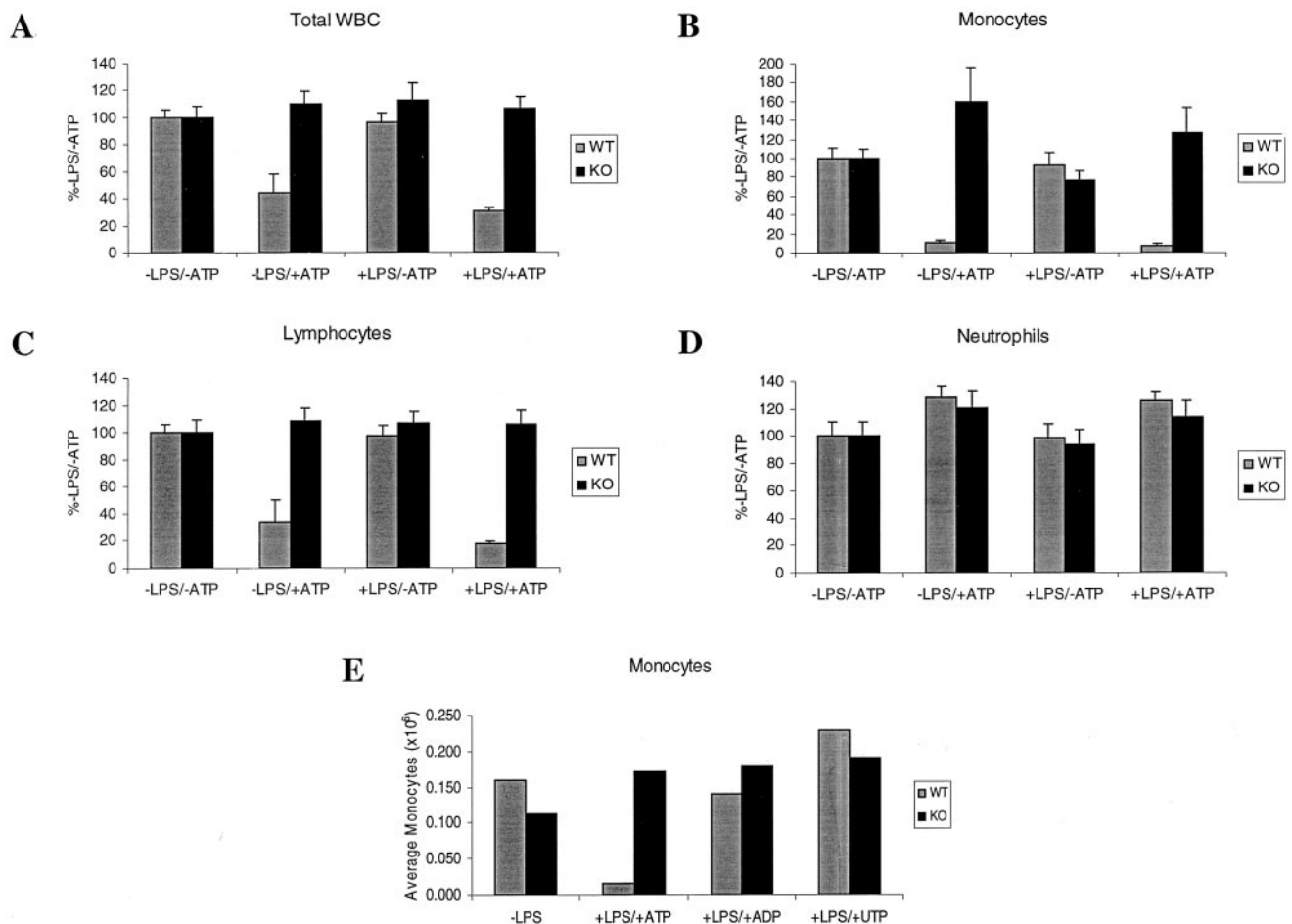


**FIGURE 1.** ATP affects blood-borne leukocyte physical properties. Blood samples from wild-type (WT) and P2X<sub>7</sub>R-deficient KO mice were treated with the indicated effector and then subjected to laser flow analysis. The graphs show results corresponding to total white blood cells (A), monocytes (B), lymphocytes (C), and neutrophils (D). Results are expressed as a percentage relative to the control sample (–LPS/–ATP) and are the mean and SE of three independent experiments. In a separate analysis, blood samples were treated with LPS and then challenged with 5 mM ATP, ADP, or UTP after which monocyte numbers were assessed (E).

lymphocytes from wild-type mice experience a morphology change and/or die in response to ATP via a P2X<sub>7</sub>R-mediated process. In contrast, no change in the number of neutrophils following ATP challenge was observed in blood samples from either wild-type or P2X<sub>7</sub>R-deficient animals (Fig. 1D). Therefore, neutrophils either lack surface expression of the P2X<sub>7</sub>R and/or fail to respond to extracellular ATP in a detectable manner.

#### Blood-based IL-1 response

Following LPS treatment of human blood, extracellular IL-1 $\beta$  can be detected but levels of the cell-dissociated cytokine increase markedly following subsequent treatment with exogenous ATP (44). To determine whether murine blood samples demonstrate a similar requirement for a secretory stimulus and to assess how the absence of the P2X<sub>7</sub>R affects IL-1 production capacity, blood samples from wild-type and P2X<sub>7</sub>R-deficient animals were subjected to LPS/ATP challenge. These blood samples were stimulated with LPS for 3 h to allow synthesis of proIL-1 $\beta$  and then treated for an additional 2 h with or without 5 mM ATP. In the presence of LPS only, no significant IL-1 $\beta$  was detected in plasma harvested from wild-type or KO blood samples (Fig. 2A). Likewise, blood samples treated with ATP without prior LPS activation generated minimal levels of extracellular IL-1 $\beta$  (Fig. 2A). However, wild-type blood samples yielded large quantities of plasma-associated IL-1 $\beta$  following serial treatment with LPS and ATP (Fig. 2A). In contrast, blood samples from P2X<sub>7</sub>R-deficient animals yielded no significant extracellular IL-1 $\beta$  following LPS and/or ATP challenge (Fig. 2A).

Concentration requirements for ATP observed in the blood-based assay were consistent with those previously reported for the P2X<sub>7</sub>R. At 0.1 mM, ATP caused no significant extracellular accumulation of IL-1 $\beta$  from LPS-activated wild-type blood (Fig. 2B). However, increasing the ATP concentration to 0.5 mM generated extracellular cytokine. Increasing the ATP concentration further to 2 mM led to additional extracellular cytokine, and higher

ATP concentrations produced a comparable response (Fig. 2B). All tested ATP concentrations were unable to promote IL-1 externalization from LPS-activated blood derived from P2X<sub>7</sub>R-deficient animals (Fig. 2B). Benzoylbenzoyl-ATP, an alternate ligand for the P2X<sub>7</sub>R (1), also promoted externalization of IL-1 $\beta$  from LPS-activated blood samples derived from wild-type animals (Fig. 2B). Although benzoylbenzoyl-ATP often acts as a more potent agonist of the P2X<sub>7</sub>R than ATP (45), in the blood-based assay this enhanced potency was not observed. The free concentration of benzoylbenzoyl-ATP is likely reduced by binding to serum proteins, and this may affect potency. Importantly, LPS-activated blood from P2X<sub>7</sub>R-deficient animals did not externalize IL-1 $\beta$  in response to benzoylbenzoyl-ATP challenge (Fig. 2B).

#### L-Selectin shedding in response to ATP is absent in P2X<sub>7</sub>R-deficient animals

Extracellular ATP is known to promote L-selectin shedding from human lymphocytes (41, 46, 47). To demonstrate that this process is P2X<sub>7</sub>R dependent, blood samples from wild-type and KO animals were treated with ATP, after which they were analyzed by FACs for leukocyte surface L-selectin expression. In this analysis, enriched T and B cell populations were distinguished based on costaining with anti-CD3 and anti-CD45, respectively, whereas monocytes and neutrophils were identified based on their distinct forward scatter properties. Monocytes, T cells, B cells, and neutrophils all stained positive for L-selectin, and no marked difference was observed in the intensity of staining between matched cell types derived from wild-type and KO animals (Table I).

A focused analysis on T cells (CD3<sup>+</sup>) yielded a clear difference in the behavior of wild-type and P2X<sub>7</sub>R-deficient counterparts. Before ATP activation, >90% of T cells isolated from wild-type animals stained positive for L-selectin. However, following 15 min of ATP exposure the percentage of L-selectin-positive T cells decreased to 18% (Fig. 3A and Table I). T cells that responded to

**FIGURE 2.** Blood-based IL-1 $\beta$  production assay. Samples of blood from wild-type (WT) and P2X<sub>7</sub>R-deficient (KO) mice were incubated for 3 h in the absence (-) or presence (+) of LPS after which they were incubated for an additional 2 h in the absence or presence of 5 mM ATP. Plasma supernatants then were isolated and the quantity of IL-1 $\beta$  present was determined by ELISA; IL-1 $\beta$  content as a function of treatment (average of triplicates) is indicated in A. This experiment was replicated three times. LPS-activated blood samples were treated for 2 h with the indicated concentration of ATP or benzoylbenzoyl-ATP (BB-ATP), and the amount of IL-1 $\beta$  released to the plasma was determined by ELISA. The quantity of IL-1 $\beta$  is indicated as a function of the effector concentration in B; each data point is the average of duplicate determinations. This experiment was replicated twice.

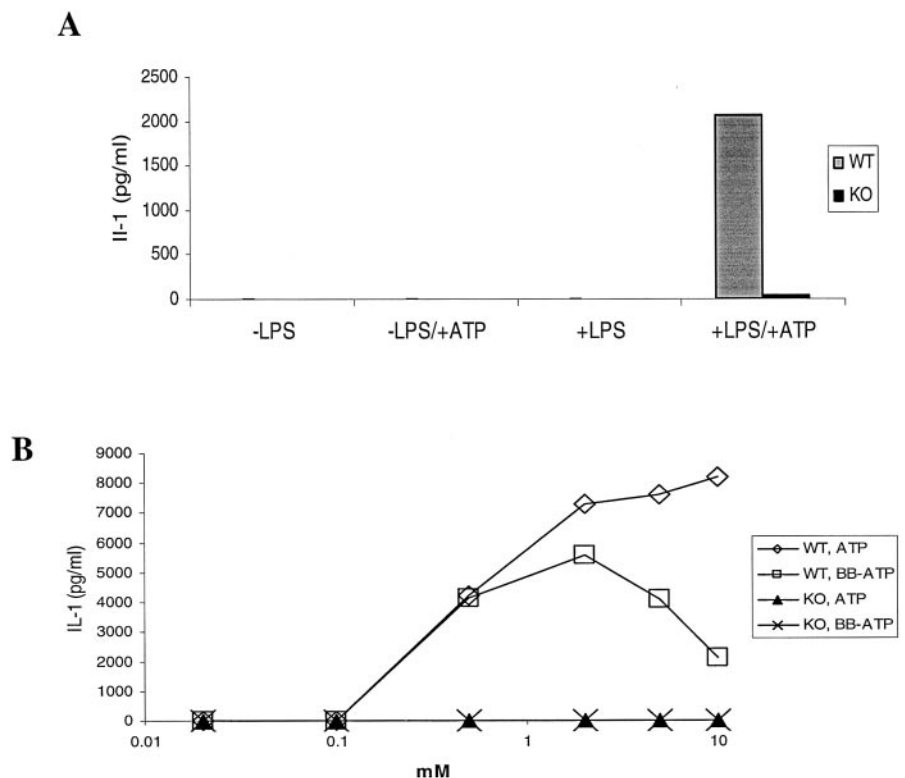


Table I. ATP-induced L-selectin shedding requires the P2X<sub>7</sub>R<sup>a</sup>

Cells	Wild Type Mice				P2X <sub>7</sub> R-Deficient Mice			
	High-intensity peak		Low-intensity peak		High-intensity peak		Low-intensity peak	
	Gating (%)	Median intensity	Gating (%)	Median intensity	Gating (%)	Median intensity	Gating (%)	Median intensity
CD3 <sup>+</sup> cells								
-ATP	92	840	— <sup>b</sup>	—	93	830	—	—
+ATP	18	900	78	7	90	800	—	—
CD45 <sup>+</sup> cells								
-ATP	84	550	—	—	86	520	—	—
+ATP	32	430	68	26	85	510	—	—
Monos								
-ATP	67	920	—	—	80	1200	—	—
+ATP	23	870	76	9	80	1100	—	—
PMNs								
-ATP	97	310	—	—	99	550	—	—
+ATP	99	640	—	—	97	780	—	—

<sup>a</sup> The high- and low-intensity peaks correspond to regions of L-selectin staining as indicated in Fig. 3. The percentage of the indicated cell type gating in the high- and low-intensity regions is indicated with and without ATP treatment.

<sup>b</sup> Absence of a value in the low-intensity peak indicates no discernable peak detected.

ATP and shed L-selectin, for the most part, were completely devoid of surface L-selectin Ag (evidenced by their low fluorescence intensity; Fig. 3A and Table I). In contrast, those T cells that did not respond retained their pre-ATP level of L-selectin staining. The percentage of T cells recovered from P2X<sub>7</sub>R-deficient animals staining positive for L-selectin was comparable to that seen in wild-type animals (>90%). However, after ATP treatment there was no significant decrease in the percentage of L-selectin-positive cells (Fig. 3A and Table I).

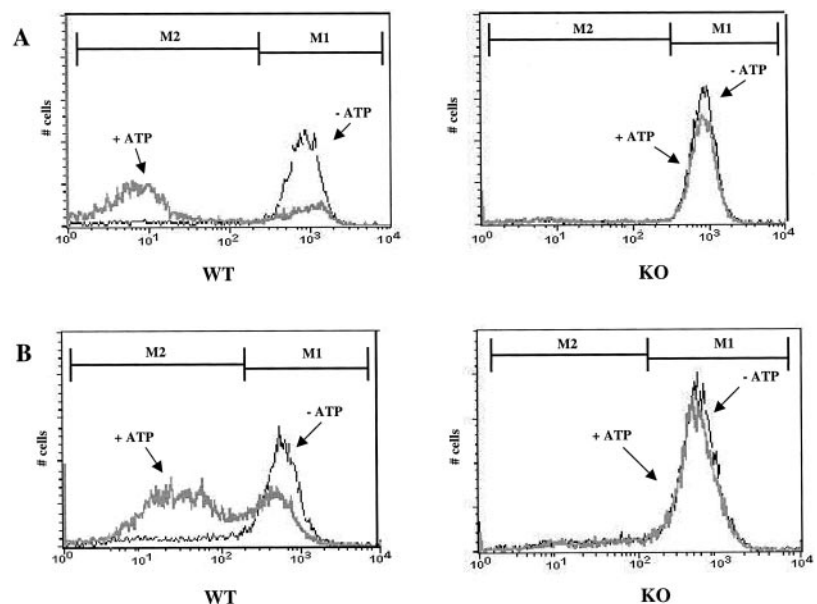
CD45<sup>+</sup> cells isolated from wild-type animals also shed L-selectin in response to ATP (Fig. 3B and Table I). In this case, 84% of the CD45<sup>+</sup> cells initially stained positive for L-selectin, and the 15-min treatment with ATP caused >50% of these cells to shed L-selectin (evidenced by the shift in fluorescence intensity). However, the affected cells retained some L-selectin staining, suggesting incomplete cleavage of surface-associated lectin. Whether complete L-selectin shedding could be achieved by increasing the length of ATP exposure was not addressed. CD45<sup>+</sup> cells recovered from the P2X<sub>7</sub>R-deficient animals showed no significant L-selectin shedding (Fig. 3B and Table I). Following the 15-min treatment

with ATP, blood samples from wild-type animals also demonstrated a 66% reduction in the number of L-selectin-positive monocytes, and the responding cells appeared to lose all surface Ag (Table I). Blood samples from the P2X<sub>7</sub>R-deficient animals, in contrast, demonstrated no decrease in monocyte-associated L-selectin staining following ATP treatment (Table I). Finally, neutrophils recovered from both wild-type and P2X<sub>7</sub>R-deficient animals showed no loss of L-selectin when challenged with ATP (Table I).

#### Morphology changes associated with P2X<sub>7</sub>R activation

Prolonged (>15 min) ligation of the P2X<sub>7</sub>R is reported to cause cell death and dramatic morphology changes in monocytes/macrophages (5, 26, 27, 48). To confirm the role of the P2X<sub>7</sub>R in mediating these effects, peritoneal macrophages from wild-type and receptor-deficient animals were isolated and treated sequentially with LPS and ATP. Wild-type macrophages treated with LPS were heterogeneous in appearance; many were firmly attached to the plastic tissue culture dishes, allowing their nuclei and intracellular architecture to be readily visualized while others were

**FIGURE 3.** FACS analysis of L-selectin shedding from blood-borne leukocytes. Blood samples from wild-type (WT) and P2X<sub>7</sub>R-deficient (KO) mice were treated for 15 min with (+) or without (-) 5 mM ATP and then subjected to FACS analysis. Enriched populations of T and B lymphocytes were distinguished based on CD3<sup>+</sup> and CD45<sup>+</sup> staining, respectively. The graphs indicate the number of CD3<sup>+</sup>-gating cells (A) and CD45<sup>+</sup>-gating cells (B) as a function of L-selectin staining intensity. Regions corresponding to the high (M<sub>1</sub>)- and low (M<sub>2</sub>)-intensity peaks listed in Table I are indicated. This experiment was repeated twice with comparable results.



rounded and nonadherent (Fig. 4). LPS-treated macrophages isolated from  $P2X_7R$ -deficient animals demonstrated similar morphological attributes (Fig. 4). However, following treatment with ATP, dramatic differences in appearance were observed between the  $P2X_7R^{+/+}$  and  $P2X_7R^{-/-}$  macrophages. After a brief 5-min exposure to ATP no significant changes were evident in either culture, but following 15 min of treatment many wild-type macrophages demonstrated loss of cytoplasmic density and their nuclei became very pronounced (Fig. 4). Increasing the ATP treatment to 30 min caused the majority of wild-type macrophages to demonstrate loss of cytoplasmic density and to appear swollen; most of these cellular corpses detached from the plastic surface. In sharp contrast, ATP-treated  $P2X_7R^{-/-}$  macrophages retained their normal morphological appearance (Fig. 4).

To determine whether the morphology change correlated with loss of cytoplasmic latency, cells and medium were harvested separately after ATP treatment and assessed for their content of the lysosomal marker enzyme  $\beta$ -hexosaminidase. An increase in extracellular  $\beta$ -hexosaminidase already was detected after 5 min of ATP treatment in wild-type cultures, and extracellular levels of this enzyme continued to increase throughout the initial 45-min treatment period (Fig. 5). At this time, 64% of the total culture-associated enzyme activity was present in the medium (Fig. 5). Importantly, cultures of LPS-treated macrophages from  $P2X_7R^{-/-}$  animals showed no time-dependent release of  $\beta$ -hexosaminidase to the medium during a 60-min incubation with ATP (Fig. 5).

#### mAb-induced arthritis

Collagen-induced arthritis in mice is a commonly used inflammatory disease model. However, the  $P2X_7R$  deficiency is established on a mixed genetic background, and such a strain is not likely to be susceptible to collagen-induced arthritis (49). Therefore, an alternate method was used to induce an arthritic type of disease involving injection of animals with a panel of four different mAbs

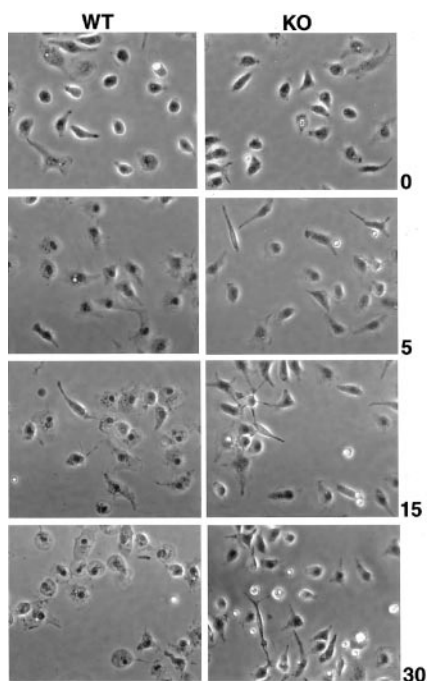


**FIGURE 4.** Morphology changes in peritoneal macrophages attendant to  $P2X_7R$  activation. Isolated peritoneal macrophages from wild-type (WT) and  $P2X_7R$ -deficient (KO) mice were stimulated with  $1 \mu\text{g/ml}$  LPS for 2 h after which they were treated with 5 mM ATP for 0, 5, 15, or 30 min. Phase contrast pictures ( $\times 40$  objective) subsequently were taken.

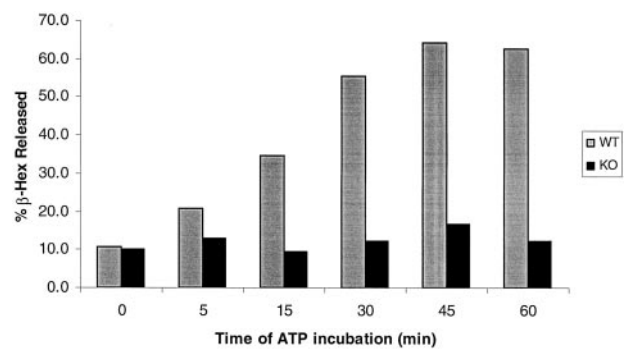
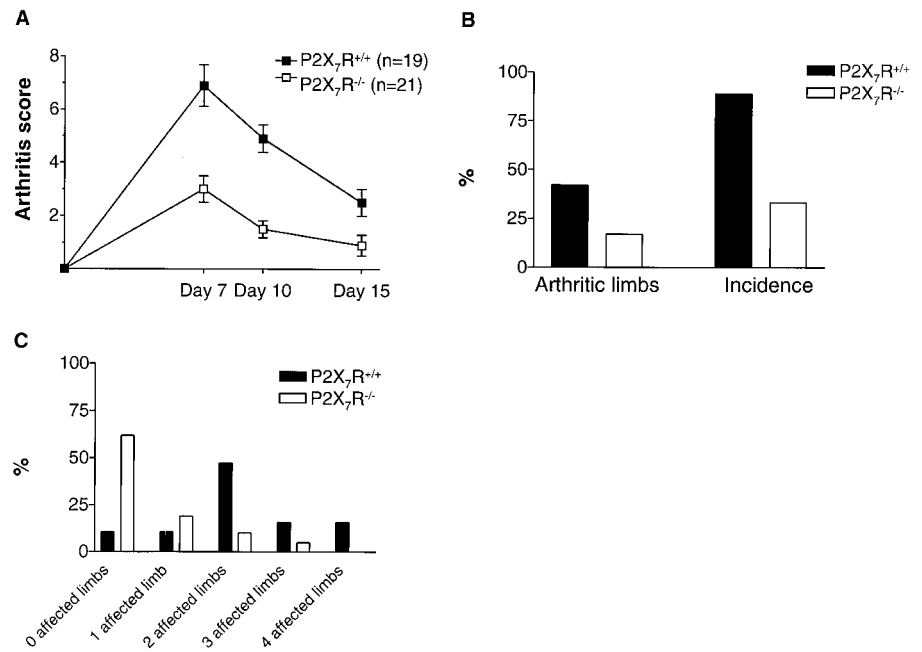


**FIGURE 5.** Activation of the  $P2X_7R$  leads to loss of plasma membrane latency. Isolated LPS-activated peritoneal macrophages from wild-type (WT) and  $P2X_7R$ -deficient (KO) mice were treated with 5 mM ATP for the indicated times, after which cells and media were harvested separately and their content of  $\beta$ -hexosaminidase was determined. The graph (results of a single experiment) shows the percentage of total culture-associated  $\beta$ -hexosaminidase recovered extracellularly as a function of treatment time.

generated against type II collagen (37, 38). One day later, the Ab-treated mice were injected with LPS and subsequently assessed for arthritis outcome measures. Gross assessment of paw swelling and inflammation indicated that the wild-type animals developed a severe arthritic phenotype within 7 days of the LPS injection (Fig. 6A). In the course of four independent experiments, the mean maximal arthritis score in the wild-type animals achieved a value near 7 (Fig. 6A). The severity of arthritis gradually declined during an additional 8 days of observation (Fig. 6A). By comparison, arthritis severity in the  $P2X_7R^{-/-}$  animals was greatly attenuated; the maximum mean score in the receptor-deficient animals was  $<3$  (Fig. 6A). Overall, the time course of the disease appeared comparable in the receptor-positive and -deficient animals (Fig. 6A). In wild-type animals, nearly 100% of the mice developed disease (Fig. 6B, Incidence), and  $>40\%$  of their limbs showed visual signs of inflammation on day 15 (Fig. 6B, arthritic limbs). In contrast,  $\sim 30\%$  of the receptor-deficient animals developed disease, and the number of affected limbs in the individual mice was reduced (Fig. 6B). Viewed in another way, the receptor-deficient population contained many animals on day 15 with few or no inflamed limbs, but the majority of the wild-type population contained two or more affected limbs (Fig. 6C).

Cartilage structural integrity also was assessed in animals subjected to mAb-induced arthritis. Groups of wild-type and receptor-deficient animals subjected to this structural analysis showed marked differences in the number of affected joints per animal (Table II). Whereas all joints in wild-type animals subjected to the mAb-induced arthritis were affected, receptor-deficient animals showed a much reduced incidence of disease (Table II). A modified Mankin score (40) was calculated based on cartilage structure, cellularity, safranin-O staining of mucopolysaccharides, and synovial inflammation/hyperplasia. In addition, to assess collagen degradation, sections were stained with a mAb (9A4) that specifically recognizes the neoepitope generated by collagenase digestion (39). Lesions observed in the articular cartilage of the stifle and hock joints recovered from wild-type animals included slight to moderate reductions in glycosaminoglycans (extending to the tidemark of the articular cartilage), which correlated inversely with increased 9A4 immunohistochemical staining (Fig. 7). Changes in cartilage cellularity, ranging from slight diffuse increases in cellularity to multifocal areas of necrosis and loss of chondrocytes, and structural changes ranging from slight surface irregularities to clefts in articular cartilage extending to the tidemark, also were

**FIGURE 6.** P2X<sub>7</sub>R-deficient animals display protection against clinical signs of mAb-induced arthritis. Wild-type (P2X<sub>7</sub>R<sup>+/+</sup>) and P2X<sub>7</sub>R-deficient (P2X<sub>7</sub>R<sup>-/-</sup>) mice were injected on sequential days with a mix of monoclonal anti-collagen Abs and LPS, after which arthritis scores were assessed. Total score as a function of days post-LPS injection is indicated in *A*; results are the mean and SD of four independent experiments ( $p < 0.05$  by two-way ANOVA). At the conclusion of the experiment (day 15), the percentage of arthritic limbs and the incidence of disease within each group of animals were determined and are indicated in *B*. Likewise, at day 15 the percentage of affected limbs displayed by animals within each genotype was determined and is indicated in *C*.



observed. In severely affected joints there was occasional slight periosteal new bone formation (data not shown). The average total modified Mankin score (and SD) in all joints from wild-type animals was calculated to be  $10.5 \pm 1.7$  (Table III). Joints from the P2X<sub>7</sub>R<sup>-/-</sup> animals displayed an overall reduction in all affected parameters, resulting in a reduced total modified Mankin score of  $5.3 \pm 4.7$  (Table III). The mean score (and SD) for 9A4 staining in stifle joints was  $2 \pm 0$  and  $0.8 \pm 1$  for wild-type and P2X<sub>7</sub>R<sup>-/-</sup> animals, respectively (Table III).

To demonstrate that P2X<sub>7</sub>R-deficient mice are capable of mounting an immune response, animals were immunized with tetanus toxoid Ag, blood samples were collected 14 days later, and the relative levels of tetanus toxoid-specific IgG in the serum were determined by ELISA. Wild-type and receptor-deficient animals possessed comparable levels of anti-tetanus toxoid IgG (Fig. 8).

## Discussion

In a previous study we provided an initial characterization of the P2X<sub>7</sub>R-deficient mouse line and demonstrated that LPS-activated peritoneal macrophages isolated from these receptor-deficient animals are incapable of processing proIL-1 $\beta$  in response to ATP challenge (31). The current study extends our initial findings by showing that blood leukocytes isolated from wild-type animals, but not P2X<sub>7</sub>R-deficient animals, adopt altered morphological and/or viability states, shed L-selectin, and generate extracellular IL-1 $\beta$  in response to ATP challenge. Moreover, we demonstrate that the severity of mAb-induced arthritis is attenuated in the receptor-deficient animals relative to that achieved in their wild-type

counterparts. These findings provide additional evidence that the P2X<sub>7</sub>R is an important regulator of inflammatory cell function, and suggest that levels of ATP generated endogenously as a result of an inflammatory response are sufficient to engage this unusual ligand-gated ion channel.

Human blood monocytes and lymphocytes are reported to express cell surface-associated P2X<sub>7</sub>Rs, and these receptors appear functionally competent as judged by the ability of the cells to alter their shape and/or volume and to accumulate fluorescent tracer molecules following ATP challenge (6, 41–44). Human neutrophils also are reported to possess the P2X<sub>7</sub>R, but the majority of their receptors appear to reside intracellularly (41). However, a recent study reported that neutrophils do respond to extracellular ATP via the P2X<sub>7</sub>R (50). Murine blood leukocytes demonstrate ATP-induced changes in cell size/shape that are consistent with previously reported patterns of P2X<sub>7</sub>R expression observed in human blood leukocytes. When blood samples from wild-type mice were treated with ATP, both lymphocytes and monocytes responded, as evidenced by the reduction in the numbers of these cells detected by laser flow analysis. Importantly, the ATP response was observed in the absence and presence of LPS prestimulation, indicating that the receptor is present and functional on resting blood-borne leukocytes. Murine blood-borne neutrophils demonstrated no discernable change in volume/shape in response to ATP challenge.

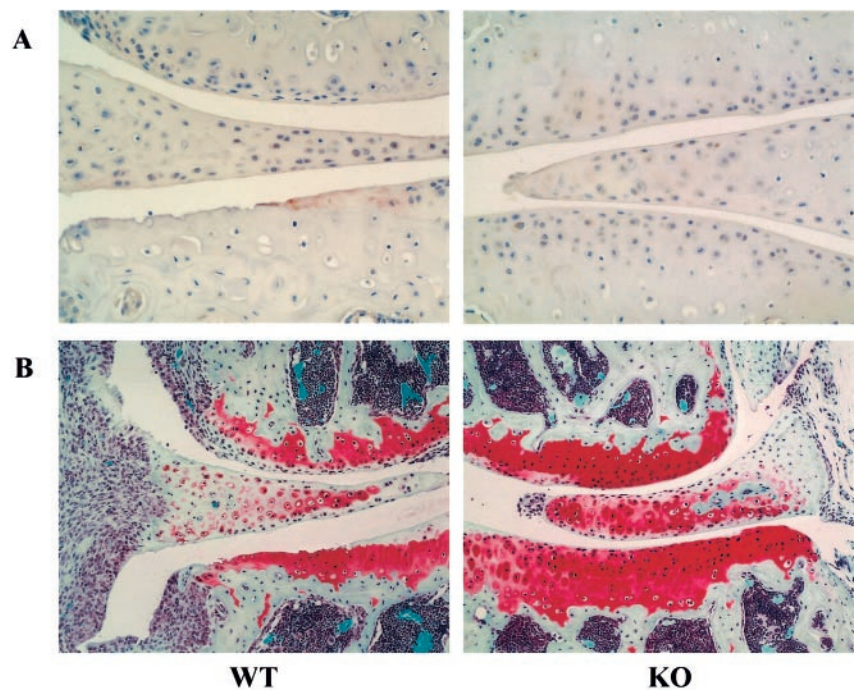
The leukocyte composition of blood samples derived from P2X<sub>7</sub>R-deficient mice was not dissimilar to that found in wild-type animals with respect to the presence of the four major cell types; however, a detailed analysis of individual T cell populations has not yet been performed. Despite this similarity in steady-state leukocyte populations, ATP-challenged P2X<sub>7</sub>R-deficient leukocytes demonstrated complete tolerance to the nucleoside triphosphate; therefore, the observed decrease in the number of wild-type leukocytes following ATP treatment is attributed to the presence of the P2X<sub>7</sub>R. Whether the decline in leukocyte numbers detected by laser flow analysis is due to an actual loss of cells or to a shape/volume change that causes the affected cell to move out of a predetermined gating window is presently unknown. However, ATP treatment of isolated mouse lymphocytes is known to cause cell death (51), and P2X<sub>7</sub>R-mediated apoptosis is observed in other cell

Table II. *Histochemical comparison of the number of affected joints in wild-type and receptor-deficient animals following mAb-induced arthritis<sup>a</sup>*

Animals	No. of Affected Joints Per Animal				
	0	1	2	3	4
+/+	0/7	0/7	0/7	0/7	7/7
-/-	0/4	1/4	1/4	1/4	1/4

<sup>a</sup> Data represent the number of affected animals/total animals in each treatment group.

**FIGURE 7.** P2X<sub>7</sub>R-deficient animals demonstrate less severe cartilage destruction following mAb-induced arthritis. Limbs from wild-type (WT) and P2X<sub>7</sub>R-deficient (KO) mice showing clinical signs of arthritis 15 days post-LPS injection were fixed and cartilage sections were characterized by histochemical analysis. Staining with the mAb 9A4 to detect the presence of a collagen cleavage neopeptide is shown in A. Sections from wild-type animals showed areas of extensive 9A4 staining (brown deposit), but the staining in sections from KO animals was generally less intense and more diffuse. Likewise, differences were observed in the intensity of staining with safranin-O, a measure of proteoglycan content (B). Sections derived from wild-type animals showed extensive areas depleted of safranin-O-positive proteoglycan extending to the tidemark. Sections from KO animals, in contrast, showed reduced areas of proteoglycan depletion. Also, sections from wild-type animals consistently showed an increased cellularity suggestive of an influx of immune cells into the synovium; fewer of these invading cells were observed in sections derived from KO animals. Sections subjected to the 9A4 and safranin-O staining are not serial sections but are derived from the same affected cartilage specimens.



systems (26, 52). Moreover, analysis of isolated peritoneal macrophages provided a dramatic example of the ability of ATP to mediate morphology changes and cell death. Wild-type peritoneal macrophages, but not those from P2X<sub>7</sub>R<sup>-/-</sup> animals, responded to extracellular ATP and underwent a rapid morphological change marked by loss of substratum adherence, clearing of the cytoplasm, and extensive swelling. This dramatic transition in cell morphology was complete within 30 min of ATP addition and coincided temporally with loss of plasma membrane latency as measured by the release of the lysosomal enzyme  $\beta$ -hexosaminidase. Therefore, ATP-induced macrophage death is accompanied by changes (e.g., swelling and release of cytosolic elements) not typically associated with an apoptotic process; this type of cell death demonstrates attributes of oncosis (53).

In response to LPS, murine blood samples failed to generate significant levels of extracellular IL-1 $\beta$ . However, following a sequential two-step activation process with LPS and ATP, large quantities of IL-1 $\beta$  were generated by wild-type, but not P2X<sub>7</sub>R<sup>-/-</sup>, blood samples. Thus, mouse blood is even more dependent on the presence of a secretory stimulus such as ATP than is human blood. With the latter, LPS alone is sufficient to promote synthesis and externalization of some IL-1 $\beta$ , but the subsequent addition of ATP to the LPS-treated samples increases the amount of externalized cytokine 10- to 30-fold (44). Murine blood samples, in contrast, generated no significant extracellular IL-1 $\beta$  in the

absence of the ATP stimulus. Like the human system, ATP treatment without prior LPS exposure generated no cell-dissociated IL-1 $\beta$ ; LPS is needed to initiate proIL-1 $\beta$  synthesis. LPS-activated blood samples derived from P2X<sub>7</sub>R<sup>-/-</sup> animals generated no cell-dissociated IL-1 $\beta$  in the presence of ATP, confirming that the export process is dependent on the P2X<sub>7</sub>R. We previously demonstrated that peritoneal macrophages isolated from wild-type and P2X<sub>7</sub>R-deficient animals respond to LPS to generate similar quantities of cell-associated proIL-1 $\beta$ . However, in response to exogenous ATP challenge, LPS-treated macrophages from wild-type animals, but not from receptor-deficient animals, released mature IL-1 $\beta$  to the medium (31). Therefore, even within the context of a complex mixture of blood proteins and blood cells, efficient generation of cell-dissociated IL-1 $\beta$  requires a secretory stimulus, and ATP working via the P2X<sub>7</sub>R can serve in this capacity.

Shedding of L-selectin from the surface of ATP-treated human lymphocytes is reported to be a P2X<sub>7</sub>R-dependent response based

Table III. Tabulation of Mankin scores

Animals	Structure	Cellularity	Safranin-O	Synovium	Total	9A4 <sup>a</sup>
+/+ (n = 7)						
Average	2.9	3.0	2.1	2.3	10.5	2.0
SD	1.2	0.0	0.3	0.8	1.7	0.0
-/- (n = 4)						
Average	1.4	1.6	1.3	1.0	5.3	0.8
SD	1.4	1.5	1.1	1.2	4.7	1.0

<sup>a</sup> Immunohistochemistry for cleavage of type II collagen was assessed using the 9A4 mAb. These values were not included in the calculation of the Mankin score but are included for comparison.

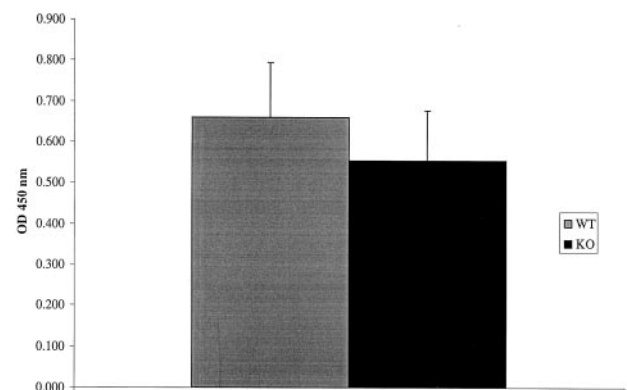


**FIGURE 8.** Wild-type and P2X<sub>7</sub>R-deficient animals mount a comparable immune response to tetanus toxoid. Serum samples were obtained from mice that had been immunized with tetanus toxoid 14 days earlier, and the quantity of toxoid-specific IgG was determined in an ELISA type of assay. OD<sub>450</sub> readings obtained at a 10,000-fold dilution of the sera are indicated for the two mouse lines; each bar corresponds to the mean and SD of 10 individual animals of each genotype.

on the required ATP concentrations, the ability of benzoylbenzoyl-ATP to substitute as the agonist, and the effect of receptor antagonists (46). Our findings demonstrating that ATP-induced L-selectin shedding is absent in leukocytes isolated from P2X<sub>7</sub>R-deficient animals confirms that the P2X<sub>7</sub>R is a necessary component of this response. Within the CD3<sup>+</sup> T cell population, the majority of cells expressed L-selectin and responded to a 15-min treatment of ATP by shedding essentially all of their surface Ag. The majority of CD45<sup>+</sup> cells also expressed L-selectin. However, following a 15-min treatment with ATP, a subset of these cells (32%) retained their full complement of L-selectin and those that did shed Ag did so incompletely. Therefore, the B cell-enriched fraction appears to be less responsive than T cells to ATP-induced L-selectin shedding. Comparison of matched leukocyte populations isolated from wild-type and receptor-deficient animals showed no significant differences in the resting levels of L-selectin surface expression, suggesting that ATP-induced L-selectin shedding does not take place during the normal circulation of leukocytes.

ATP-induced responses demonstrated by wild-type leukocytes (i.e., cell activation/death, IL-1 $\beta$  production, and L-selectin shedding) are expected to impact the outcome of an inflammatory response. Indeed, in response to mAb-induced arthritis, P2X<sub>7</sub>R-deficient animals demonstrated reduced susceptibility and severity of disease relative to their wild-type counterparts. This resistance manifested as less swelling and redness of affected joints and less destruction of cartilage. In wild-type animals, the mAb stimulus led to a phenotype not dissimilar to that observed in collagen-induced arthritis in terms of both quantitative and qualitative changes (49, 54). This latter model is dependent on IL-1, and inhibitors of the production and/or activity of this cytokine suppress disease outcomes (55, 56). At the histological level, mAb-induced arthritis led to a disruption of the normal cartilage architecture, loss of proteoglycan content, synovial inflammation, and the appearance of collagen cleavage products as detected with the mAb 9A4 (39). The time required to achieve disease in the monoclonal arthritis model is reduced relative to that required in the collagen-induced model, but the severity of the disease appears comparable in the two formats. All assessed histological changes were less severe in the P2X<sub>7</sub>R-deficient animals relative to those observed in matched wild-type controls. This suggests that the absence of the P2X<sub>7</sub>R leads to a general suppression of the inflammatory response, perhaps reflecting a diminished output of inflammatory mediators such as IL-1. Importantly, wild-type and receptor-deficient animals were equally competent in their response to tetanus-toxoid Ag; this type of an immune response requires Ag presentation, Th cell function, and B cell Ab production. Thus, P2X<sub>7</sub>R-deficient animals are not generally immunocompromised.

To date, no activity has been reported for the P2X<sub>7</sub>R that does not involve ligand-induced activation of the channel/pore. Therefore, demonstration that absence of the P2X<sub>7</sub>R alters disease outcome in an in vivo model of inflammation suggests that this receptor encounters sufficient levels of an endogenous ligand to promote its activation in wild-type animals. This is an important finding, as previous in vivo studies investigating this receptor have used exogenous ATP as the activating ligand (31). In the mAb-induced arthritis model no exogenous ATP was introduced, so receptor activation must result from the presence of an appropriate endogenous ligand. Whether ATP is released to local environments where its concentration can achieve levels sufficient to activate the receptor, or whether other endogenous effectors can lower ATP concentration requirements remains to be established.

## References

- Surprenant, A., F. Rassendren, E. Kawashima, R. A. North, and G. Buell. 1996. The cytolitic P2Z receptor for extracellular ATP identified as a P2X receptor (P2X<sub>7</sub>). *Science* 272:735.
- Michel, A. D., I. P. Chessell, A. D. Hibell, J. Simon, and P. P. Humphrey. 1998. Identification and characterization of an endogenous P2X<sub>7</sub> (P2Z) receptor in CHO-K1 cells. *Br. J. Pharmacol.* 125:1194.
- Chessell, I. P., J. Simon, A. D. Hibell, A. D. Michel, E. A. Barnard, and P. P. Humphrey. 1998. Cloning and functional characterisation of the mouse P2X<sub>7</sub> receptor. *FEBS Lett.* 439:26.
- North, R. A. 1996. Families of ion channels with two hydrophobic segments. *Curr. Opin. Cell Biol.* 8:474.
- Steinberg, T. H., A. S. Newman, J. A. Swanson, and S. C. Silverstein. 1987. ATP<sup>4-</sup> permeabilizes the plasma membrane of mouse macrophages to fluorescent dyes. *J. Biol. Chem.* 262:8884.
- Hickman, S. E., J. el Khoury, S. Greenberg, I. Schieren, and S. C. Silverstein. 1994. P2Z adenosine triphosphate receptor activity in cultured human monocyte-derived macrophages. *Blood* 84:2452.
- Virginio, C., A. MacKenzie, R. A. North, and A. Surprenant. 1999. Kinetics of cell lysis, dye uptake and permeability changes in cells expressing the rat P2X<sub>7</sub> receptor. *J. Physiol.* 519:335.
- Buisman, H. P., T. H. Steinberg, J. Fischbar, S. C. Silverstein, S. A. Vogelzang, C. Ince, D. L. Ypey, and P. C. Leijh. 1988. Extracellular ATP induces a large nonselective conductance in macrophage plasma membranes. *Proc. Natl. Acad. Sci. USA* 85:7988.
- Ferrari, D., P. Chiozzi, S. Falzoni, M. Dal Susino, G. Collo, G. Buell, and F. Di Virgilio. 1997. ATP-mediated cytotoxicity in microglial cells. *Neuropharmacology* 36:1295.
- Khakh, B. S., X. R. Bao, C. Labarca, and H. A. Lester. 1999. Neuronal P2X transmitter-gated cation channels change their ion selectivity in seconds. *Nat. Neurosci.* 2:322.
- Virginio, C., A. MacKenzie, F. A. Rassendren, R. A. North, and A. Surprenant. 1999. Pore dilation of neuronal P2X receptor channels. *Nat. Neurosci.* 2:315.
- Rassendren, F., G. N. Buell, C. Virginio, G. Collo, R. A. North, and A. Surprenant. 1997. The permeabilizing ATP receptor, P2X<sub>7</sub>: cloning and expression of a human cDNA. *J. Biol. Chem.* 272:5482.
- Schilling, W. P., T. Wasylina, G. R. Dubyak, B. D. Humphreys, and W. G. Sinkins. 1999. Maitotoxin and P2Z/P2X<sub>7</sub> purinergic receptor stimulation activate a common cytolitic pore. *Am. J. Physiol.* 277:C766.
- Estacion, M., and W. Schilling. 2001. Maitotoxin-induced membrane blebbing and cell death in bovine aortic endothelial cells. *BMC Physiol.* 1:2.
- Collo, G., S. Neidhart, E. Kawashima, M. Kosco-Vilbois, R. A. North, and G. Buell. 1997. Tissue distribution of the P2X<sub>7</sub> receptor. *Neuropharmacology* 36:1277.
- Di Virgilio, F., P. Chiozzi, D. Ferrari, S. Falzoni, J. M. Sanz, A. Morelli, M. Torboli, G. Bolognesi, and O. R. Baricordi. 2001. Nucleotide receptors: an emerging family of regulatory molecules in blood cells. *Blood* 97:587.
- Apasov, S. G., M. Koshiba, T. M. Chused, and M. V. Sitkovsky. 1997. Effects of extracellular ATP and adenosine on different thymocyte subsets: possible role of ATP-gated channels and G protein-coupled purinergic receptor. *J. Immunol.* 158:5095.
- Baricordi, O. R., L. Melchiorri, E. Adinolfi, S. Falzoni, P. Chiozzi, G. Buell, and F. Di Virgilio. 1999. Increased proliferation rate of lymphoid cells transfected with the P2X<sub>7</sub> ATP receptor. *J. Biol. Chem.* 274:33206.
- Chiozzi, P., J. M. Sanz, D. Ferrari, S. Falzoni, A. Aleotti, G. N. Buell, G. Collo, and F. Di Virgilio. 1997. Spontaneous cell fusion in macrophage cultures expressing high levels of the P2Z/P2X<sub>7</sub> receptor. *J. Cell Biol.* 138:697.
- Falzoni, S., P. Chiozzi, D. Ferrari, G. Buell, and F. Di Virgilio. 2000. P2X<sub>7</sub> receptor and polykaryon formation. *Mol. Biol. Cell* 11:3169.
- Lammas, D. A., C. Stober, C. J. Harvey, N. Kendrick, S. Panchalingam, and D. S. Kumararatne. 1997. ATP-induced killing of mycobacteria by human macrophages is mediated by purinergic P2Z(P2X<sub>7</sub>) receptors. *Immunity* 7:433.
- Coutinho-Silva, R., J. L. Perfettini, P. M. Persechini, A. Dautry-Varsat, and D. M. Ojcius. 2001. Modulation of P2Z/P2X<sub>7</sub> receptor activity in macrophages infected with *Chlamydia psittaci*. *Am. J. Physiol.* 280:C81.
- Ferrari, D., S. Wesselborg, M. K. Bauer, and K. Schulze-Osthoff. 1997. Extracellular ATP activates transcription factor NF- $\kappa$ B through the P2Z purinoreceptor by selectively targeting NF- $\kappa$ B p65. *J. Cell Biol.* 139:1635.
- Humphreys, B. D., J. Rice, S. B. Kerteszy, and G. R. Dubyak. 2000. Stress-activated protein kinase/JNK activation and apoptotic induction by the macrophage P2X<sub>7</sub> nucleotide receptor. *J. Biol. Chem.* 275:26792.
- Hide, I., M. Tanaka, A. Inoue, K. Nakajima, S. Kohsaka, K. Inoue, and Y. Nakata. 2000. Extracellular ATP triggers tumor necrosis factor- $\alpha$  release from rat microglia. *J. Neurochem.* 75:965.
- Hogquist, K. A., M. A. Nett, E. R. Unanue, and D. D. Chaplin. 1991. Interleukin 1 is processed and released during apoptosis. *Proc. Natl. Acad. Sci. USA* 88:8485.
- Perregaux, D., and C. A. Gabel. 1994. Interleukin-1 $\beta$  maturation and release in response to ATP and nigericin: evidence that potassium depletion mediated by these agents is a necessary and common feature of their activity. *J. Biol. Chem.* 269:15195.
- Sanz, J. M., and F. Di Virgilio. 2000. Kinetics and mechanism of ATP-dependent IL-1 $\beta$  release from microglial cells. *J. Immunol.* 164:4893.
- MacKenzie, A., H. L. Wilson, E. Kiss-Toth, S. K. Dower, R. A. North, and A. Surprenant. 2001. Rapid secretion of interleukin-1 $\beta$  by microvesicle shedding. *Immunity* 8:825.

30. Laliberte, R. E., J. Egger, and C. A. Gabel. 1999. ATP treatment of human monocytes promotes caspase-1 maturation and externalization. *J. Biol. Chem.* 274:36944.
31. Solle, M., J. Labasi, D. G. Perregaux, E. Stam, N. Petrushova, B. H. Koller, R. J. Griffiths, and C. A. Gabel. 2001. Altered cytokine production in mice lacking P2X<sub>7</sub> receptors. *J. Biol. Chem.* 276:125.
32. Beigi, R., E. Kobatake, M. Aizawa, and G. R. Dubyak. 1999. Detection of local ATP release from activated platelets using cell surface-attached firefly luciferase. *Am. J. Physiol.* 276:C267.
33. Oshimi, Y., S. Miyazaki, and S. Oda. 1999. ATP-induced Ca<sup>2+</sup> response mediated by P2U and P2Y purinoceptors in human macrophages: signalling from dying cells to macrophages. *Immunology* 98:220.
34. Schwiebert, E. M. 1999. ABC transporter-facilitated ATP conductive transport. *Am. J. Physiol.* 276:C1.
35. Verderio, C., and M. Matteoli. 2001. ATP mediates calcium signaling between astrocytes and microglial cells: modulation by IFN- $\gamma$ . *J. Immunol.* 166:6383.
36. Cornbleet, P. J., D. Myrick, S. Judkins, and R. Levy. 1992. Evaluation of the CELL-DYNE 3000 differential. *Am. J. Clin. Pathol.* 98:603.
37. Terato, K., K. A. Hasty, R. A. Reife, M. A. Cremer, A. H. Kang, and J. M. Stuart. 1992. Induction of arthritis with monoclonal antibodies to collagen. *J. Immunol.* 148:2103.
38. Terato, K., D. S. Harper, M. M. Griffiths, D. L. Hasty, X. J. Ye, M. A. Cremer, and J. M. Seyer. 1995. Collagen-induced arthritis in mice: synergistic effect of *E. coli* lipopolysaccharide bypasses epitope specificity in the induction of arthritis with monoclonal antibodies to type II collagen. *Autoimmunity* 22:137.
39. Otterness, I. G., J. T. Downs, C. Lane, M. L. Bliven, H. Stukenbrok, D. N. Scampoli, A. J. Milici, and P. S. Mezes. 1999. Detection of collagenase-induced damage of collagen by 9A4, a monoclonal C-terminal neopeptide antibody. *Matrix Biol.* 18:331.
40. Mankin, H. J., H. Dorfman, L. Lippiello, and A. Zarins. 1971. Biochemical and metabolic abnormalities in articular cartilage from osteo-arthritic human hips. II. Correlation of morphology with biochemical and metabolic data. *J. Bone Joint Surg. Am.* 53:523.
41. Gu, B. J., W. Y. Zhang, L. J. Bendall, I. P. Chessell, G. N. Buell, and J. S. Wiley. 2000. Expression of P2X<sub>7</sub> purinoceptors on human lymphocytes and monocytes: evidence for nonfunctional P2X<sub>7</sub> receptors. *Am. J. Physiol.* 279:C1189.
42. Sluyter, R., J. A. Barden, and J. S. Wiley. 2001. Detection of P2X purinergic receptors on human B lymphocytes. *Cell Tissue Res.* 304:231.
43. Gudipaty, L., B. D. Humphreys, G. Buell, and G. R. Dubyak. 2001. Regulation of P2X<sub>7</sub> nucleotide receptor function in human monocytes by extracellular ions and receptor density. *Am. J. Physiol.* 280:C943.
44. Perregaux, D. G., P. McNiff, R. Laliberte, M. Conklyn, and C. A. Gabel. 2000. ATP acts as an agonist to promote stimulus-induced secretion of IL-1 $\beta$  and IL-18 in human blood. *J. Immunol.* 165:4615.
45. el-Moatassim, C., and G. R. Dubyak. 1992. A novel pathway for the activation of phospholipase D by P2z purinergic receptors in BAC1.2F5 macrophages. *J. Biol. Chem.* 267:23664.
46. Jamieson, G. P., M. B. Snook, P. J. Thurlow, and J. S. Wiley. 1996. Extracellular ATP causes loss of L-selectin from human lymphocytes via occupancy of P2Z purinoceptors. *J. Cell Physiol.* 166:637.
47. Gu, B., L. J. Bendall, and J. S. Wiley. 1998. Adenosine triphosphate-induced shedding of CD23 and L-selectin (CD62L) from lymphocytes is mediated by the same receptor but different metalloproteases. *Blood* 92:946.
48. Falzoni, S., M. Munerati, D. Ferrari, S. Spisani, S. Moretti, and F. Di Virgilio. 1995. The purinergic P2Z receptor of human macrophage cells: characterization and possible physiological role. *J. Clin. Invest.* 95:1207.
49. Wooley, P. H., H. S. Luthra, J. M. Stuart, and C. S. David. 1981. Type II collagen-induced arthritis in mice. I. Major histocompatibility complex (I region) linkage and antibody correlates. *J. Exp. Med.* 154:688.
50. Suh, B.-C., J.-S. Kim, U. Namgung, H. Ha, and K.-T. Kim. 2001. P2X<sub>7</sub> nucleotide receptor mediation of membrane pore formation and superoxide generation in human promyelocytes and neutrophils. *J. Immunol.* 166:6754.
51. Zanollo, P., V. Bronte, A. Rosato, P. Pizzo, and F. Di Virgilio. 1990. Responses of mouse lymphocytes to extracellular ATP. II. Extracellular ATP causes cell type-dependent lysis and DNA fragmentation. *J. Immunol.* 145:1545.
52. Ferrari, D., M. Los, M. K. Bauer, P. Vandenabeele, S. Wesselborg, and K. Schulze-Osthoff. 1999. P2Z purinoceptor ligation induces activation of caspases with distinct roles in apoptotic and necrotic alterations of cell death. *FEBS Lett.* 447:71.
53. Majno, G., and I. Joris. 1995. Apoptosis, oncosis, and necrosis: an overview of cell death. *Am. J. Pathol.* 146:3.
54. Griffiths, R. J., M. A. Smith, M. L. Roach, J. L. Stock, E. J. Stam, A. J. Milici, D. N. Scampoli, J. D. Eskra, R. S. Byrum, B. H. Koller, and J. D. McNeish. 1997. Collagen-induced arthritis is reduced in 5-lipoxygenase-activating protein-deficient mice. *J. Exp. Med.* 185:1123.
55. Joosten, L. A., M. M. Helsen, T. Saxne, F. A. van De Loo, D. Heinegard, and W. B. van Den Berg. 1999. IL-1 $\alpha\beta$  blockade prevents cartilage and bone destruction in murine type II collagen-induced arthritis, whereas TNF $\alpha$  blockade only ameliorates joint inflammation. *J. Immunol.* 163:504.
56. Williams, R. O., L. Marinova-Mutafchieva, M. Feldmann, and R. N. Maini. 2000. Evaluation of TNF $\alpha$  and IL-1 blockade in collagen-induced arthritis and comparison with combined anti-TNF $\alpha$ /anti-CD4 therapy. *J. Immunol.* 165:7240.